

SUPPORTING INFORMATION

2D Wax-printed paper substrates with extended solvent supply capabilities allow enhanced ion signal in paper spray ionization

*Deidre E. Damon, Yosef S. Maher, Mengzhen Yin, Fred P. M. Jjunju, Iain S. Young, Stephen Taylor, Simon Maher, and Abraham K. Badu-Tawiah**

Supporting information is summarized in the table below

Topic	Title of Topic	Pages
Topic 1 (Figure S1,S2)	Comparison of different geometries of microfluidic channels	2
Topic 2 (Figure S3)	Comparison of s_2 , s_3 , and un-waxed paper with varying voltages	4
Topic 3 (Figure S4)	Exploration of increased ion current near the end of spray lifetime	5
Topic 4 (Figures S5, S6, S7)	Calibration curves referenced by Table 1	6
Topic 5 (Figure S8)	Total ion chromatogram for un-waxed paper using acetonitrile spray solvent	9
Topic 6 (Figure S9)	Duomeen analysis from pre- and post-treatment water samples	10
Topic 7 (Figure S10)	Metaldehyde fragmentation	11
Topic 8 (Figure S11)	Metaldehyde dissociation in acidified solution	12

1. Comparison of different geometries of microfluidic channels. As equal voltage is applied to each paper triangle pattern, available area shape and magnitude varies, which alters the charge density (given here as volt per area). When the available voltage per area was analyzed (**Fig. S1**), we predict that charge density should be greater for paper with printed wax patterns. Detail geometrical differences of all patterns is provided in **Fig. S2**.

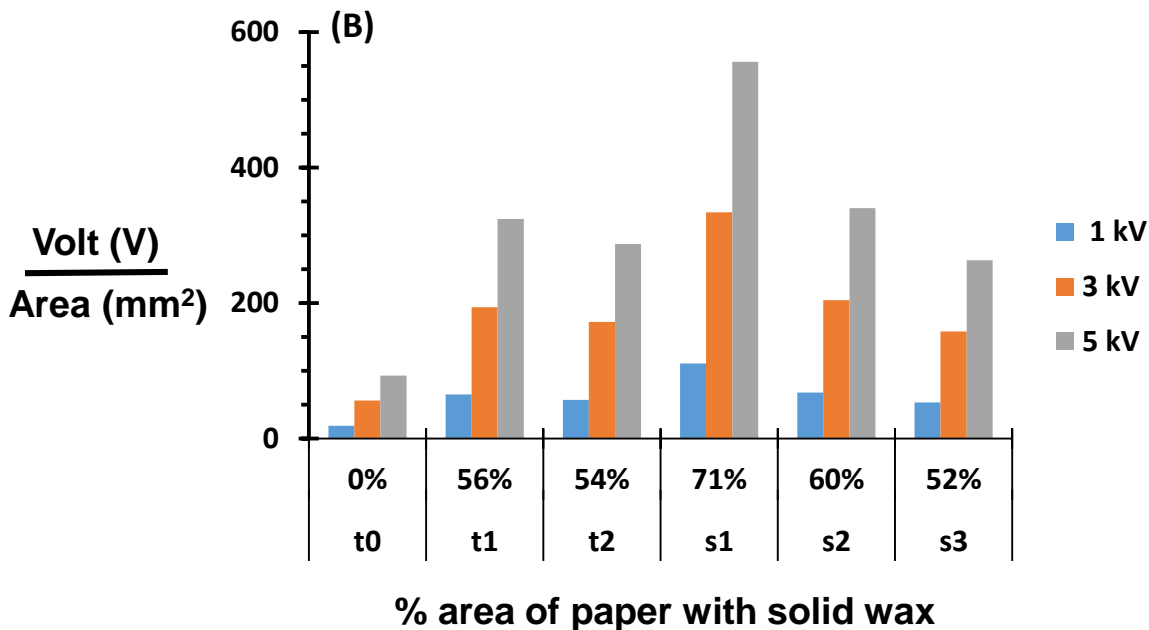


Figure S1. Charge density (V/mm²) is shown to increase as the area available to solvent decreases.

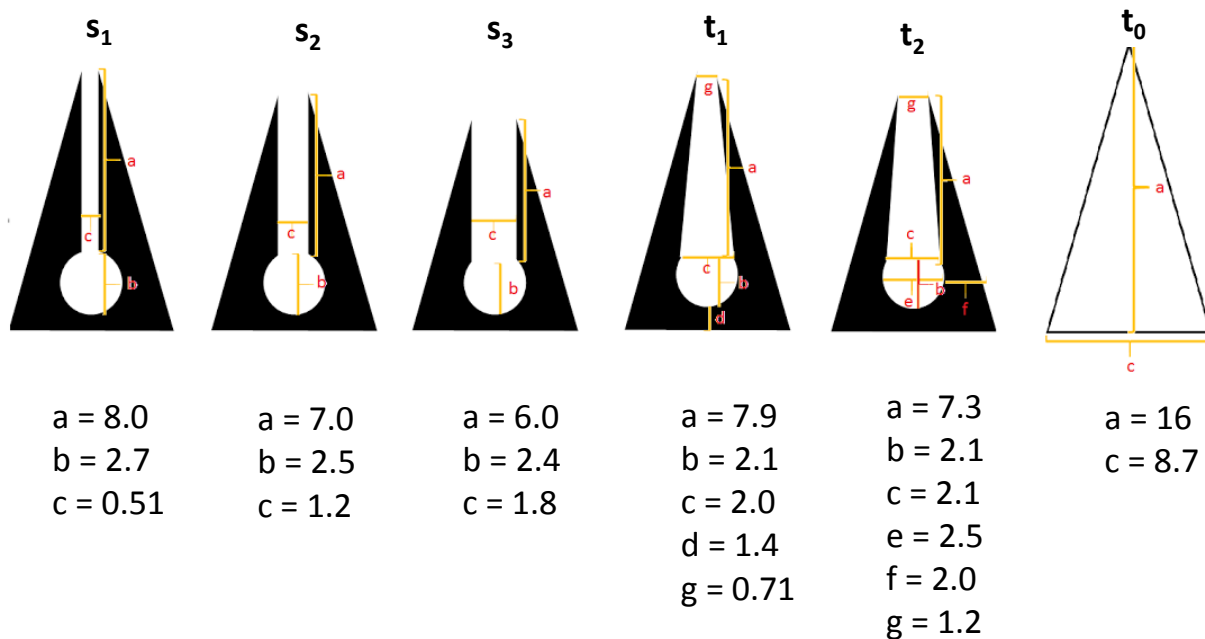


Figure S2. Detail geometrical differences between all wax-printed patterns is provided. All parameters are given in millimeters (mm). Overall geometry of all paper triangles are approximately measured 9 mm base and 16 mm height.

2. Comparison of s_2 , s_3 , and un-waxed paper. Selection of optimal wax-printed pattern was achieved by via comparison of absolute MS/MS product ion intensities of methamphetamine (m/z 150 \rightarrow 119), amphetamine (m/z 136 \rightarrow 119), and cocaine (m/z 304 \rightarrow 182) using at 0-5 kV spray voltages (**Fig. S3**). Pattern s_3 was selected for further experiments because it produced higher signal intensity than both s_2 and un-waxed paper.

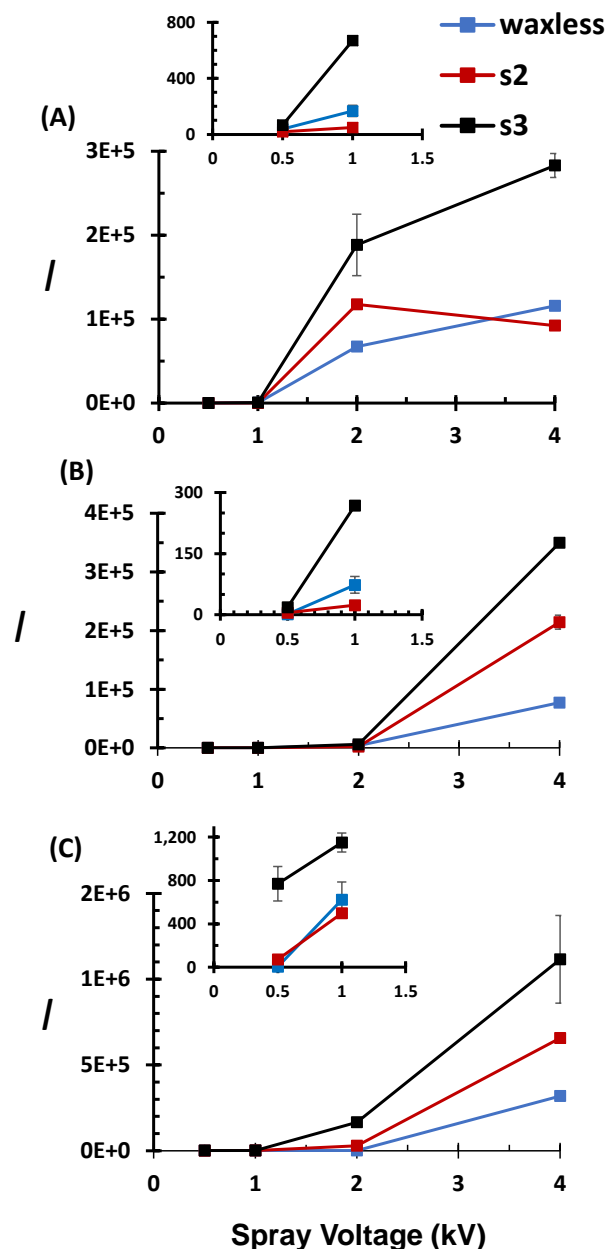


Figure S3. Comparison of s_2 , s_3 , and t_0 (waxless) paper triangles as a function of voltage using (A) amphetamine, (B) cocaine, and (C) methamphetamine diluted in water at 250 ng/mL. Error bars show standard deviation for three replicates. At all voltages, s_3 wax-printed paper substrate produced higher signal intensity than un-waxed paper. I = absolute product ion intensities.

3. Analysis of ion current. The occurrence of corona discharge in wax-printed paper spray was investigated by analyzing the redox active compound 6-methoxy-1,2,3,4-tetrahydroquinoline (MW 163). In particular, we suspected the rise in current (see total ion chromatogram (TIC) below) as result of solvent depletion might produce radical cations M^+ (m/z 163). This expectation was not met; instead all in the TIC showed only protonated species at m/z 164 (**Figure S4**). As a consequence, we concluded that the occurrence of corona discharge in the wax-printed channels is minimal.

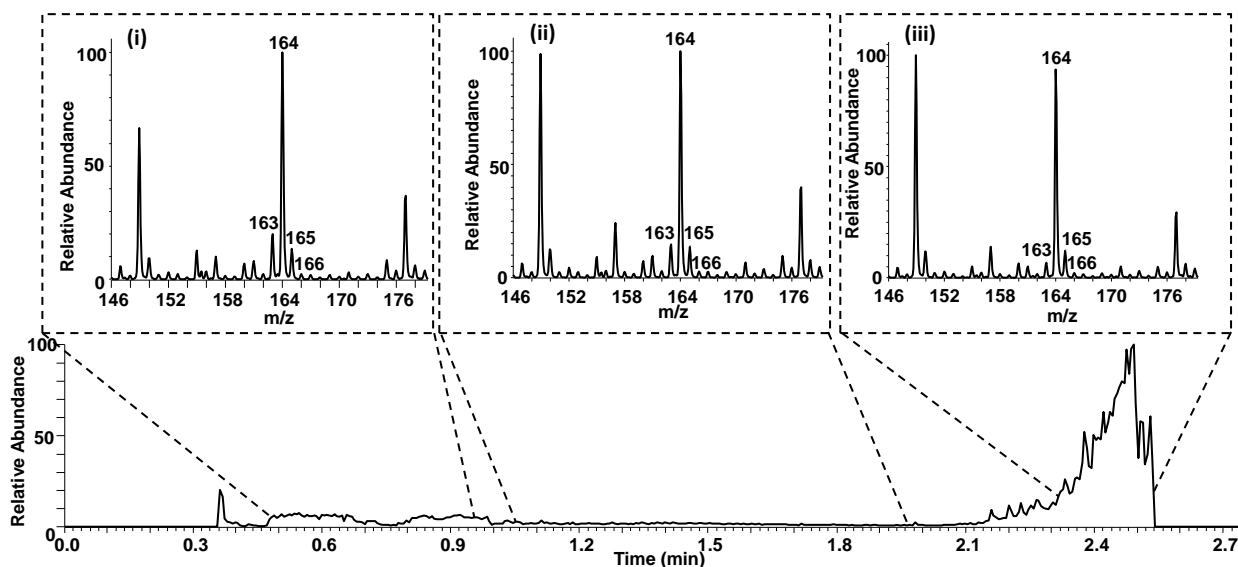


Figure S4. Total ion chromatogram recorded after spraying of 1 ppm 6-methoxy-1,2,3,4-tetrahydroquinoline with 10 μ L 4:1 MeOH/H₂O spray solvent at 3 kV. Inserts shown mass spectra taken from (i) the beginning of spray lifetime, (ii) stable spray region, and (iii) increased spray current region near the end of spray lifetime. No significant difference is seen in the mass spectra.

4. Linear calibration of drugs in urine. Concentrations of 3-500 *ng/mL* were quantified in fresh and dry urine to give LODs shown in **Table 1** (main manuscript). All samples were analyzed at 3 kV spray voltage.

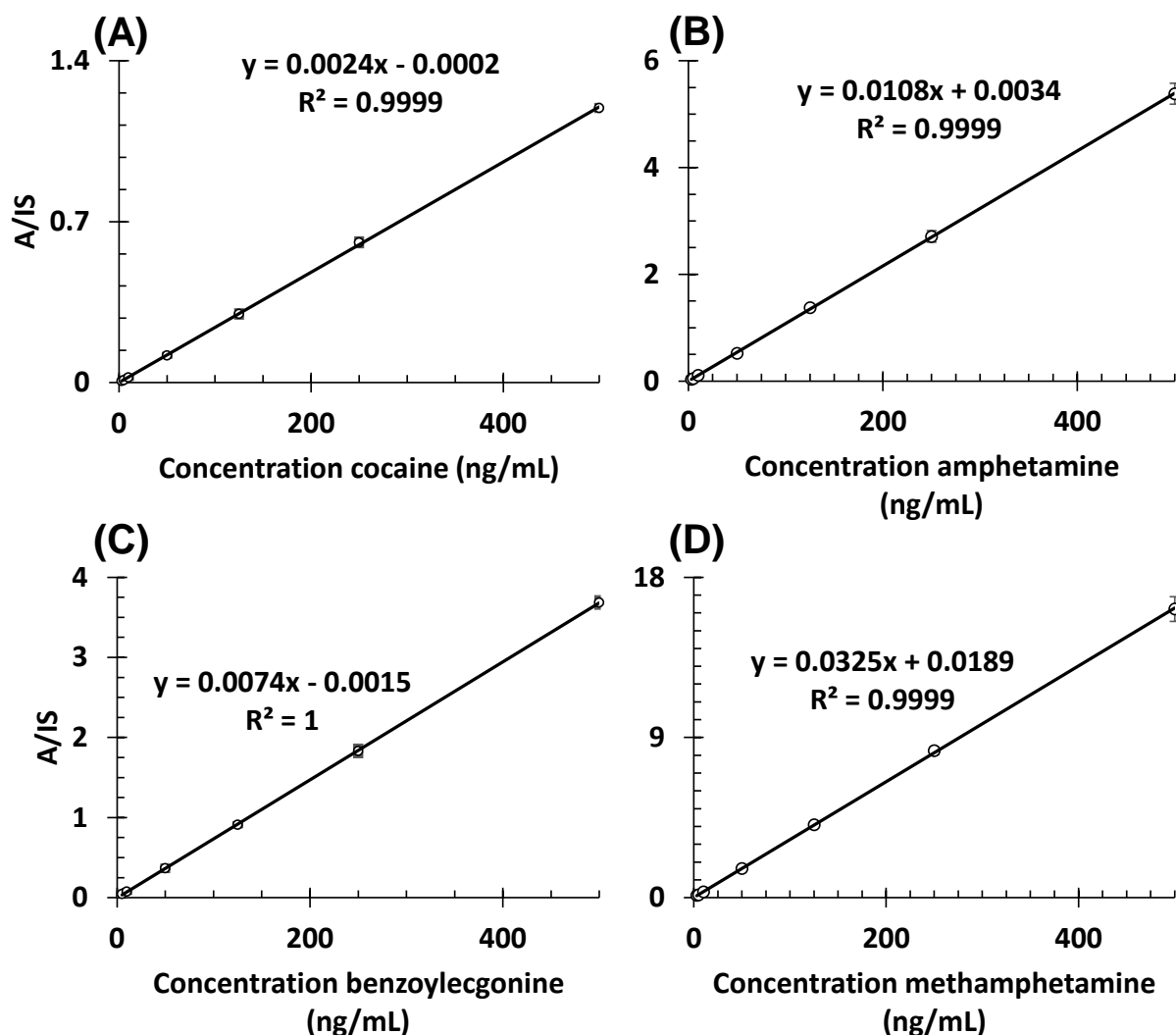


Figure S5. Samples of 4 μL fresh urine spiked with 3 – 500 *ng/mL* drug, sprayed with 10 μL of 100% acetonitrile on s_3 wax paper. Drugs were quantified with absolute intensity of fragmentation (A) divided by their respective internal standards (IS) of (A) cocaine (m/z 304 \rightarrow 182) and IS d_3 (m/z 307 \rightarrow 185), (B) amphetamine (m/z 136 \rightarrow 119) and IS d_5 (m/z 141 \rightarrow 123), (C) benzoyllecgonine (m/z 290 \rightarrow 168), and IS d_3 (m/z 293 \rightarrow 171) (D) methamphetamine (m/z 150 \rightarrow 119) and IS d_5 (m/z 155 \rightarrow 123).

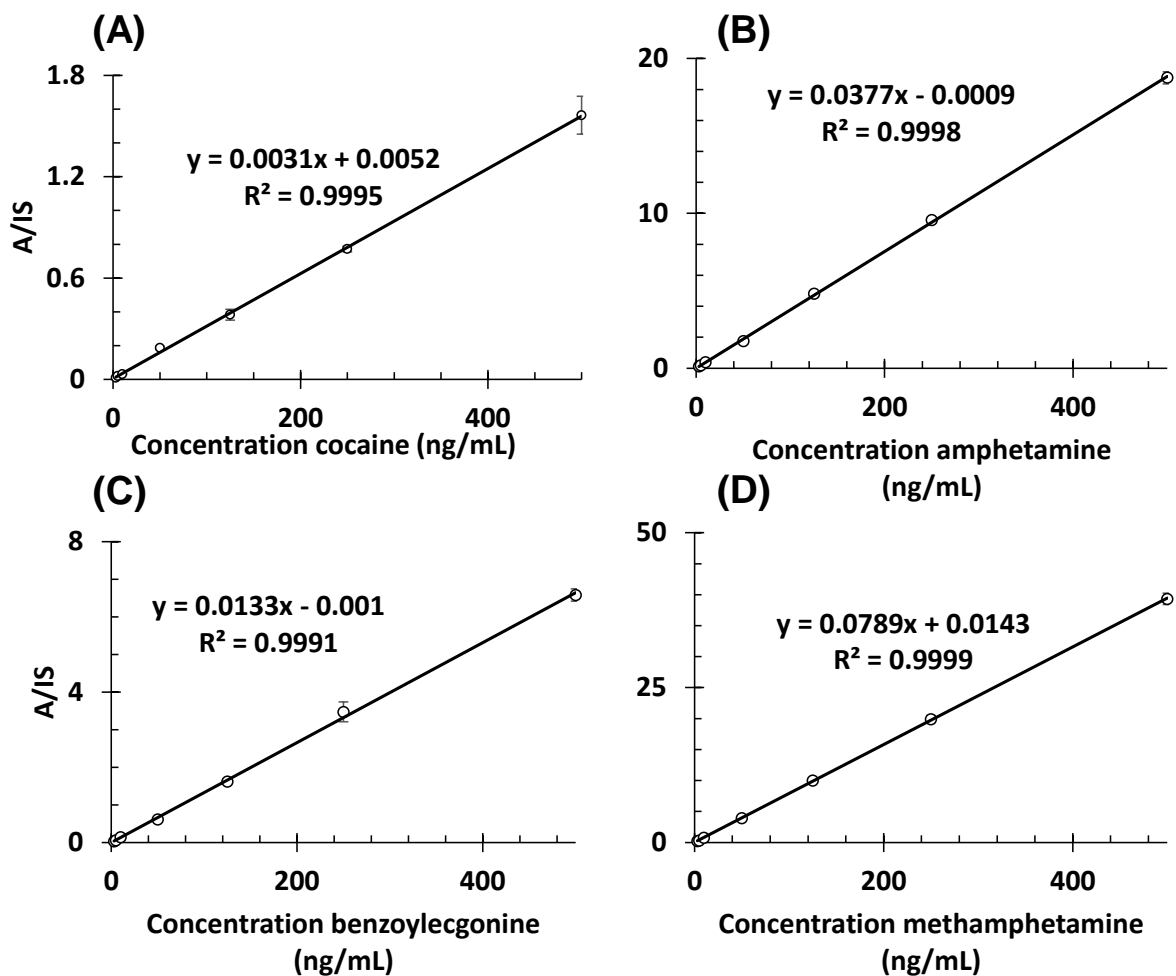


Figure S6. Samples of 4 μL dried urine spiked with 3 – 500 ng/mL drug, sprayed with 10 μL of 100% acetonitrile on s_3 wax paper. Drugs were quantified with absolute intensity of fragmentation (A) divided by their respective internal standards (IS) of **(A)** cocaine (m/z 304 \rightarrow 182) and IS d_3 (m/z 307 \rightarrow 185), **(B)** amphetamine (m/z 136 \rightarrow 119) and IS d_5 (m/z 141 \rightarrow 123), **(C)** benzoylecgonine (m/z 290 \rightarrow 168), and IS d_3 (m/z 293 \rightarrow 171) **(D)** methamphetamine (m/z 150 \rightarrow 119) and IS d_5 (m/z 155 \rightarrow 123).

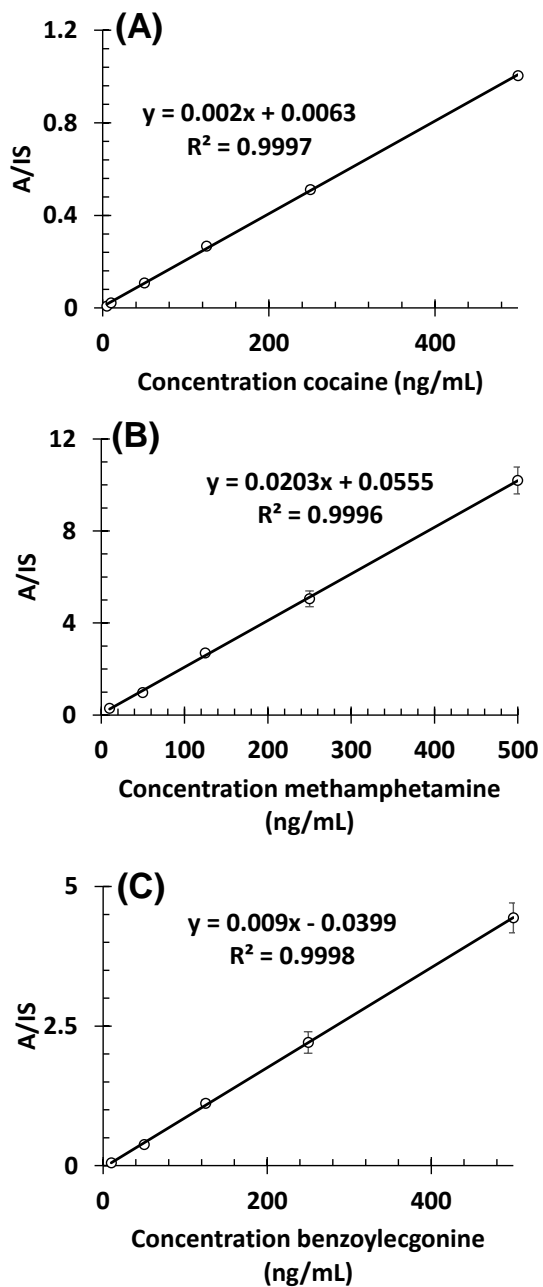


Figure S7. Samples of 4 μ L dried urine spiked with 3 – 500 ng/mL drug, sprayed with 20 μ L of 100% acetonitrile on un-waxed paper. Drugs were quantified with absolute intensity of fragmentation (A) divided by their respective internal standards (IS) of **(A)** cocaine (m/z 304 \rightarrow 182) and IS d_3 (m/z 307 \rightarrow 185), **(B)** methamphetamine (m/z 150 \rightarrow 119) and IS d_5 (m/z 155 \rightarrow 123), and **(C)** benzoylecgonine (m/z 290 \rightarrow 168), and IS d_3 (m/z 293 \rightarrow 171).

5. TIC of cocaine on un-waxed paper. Dried urine sample present on un-waxed paper was analysed with 10 μL and 20 μL pure acetonitrile. Because the spray solvent was allowed to spread over the entire paper surface, the increased surface area in contact with air accelerated evaporation, which decreased signal lifetime.

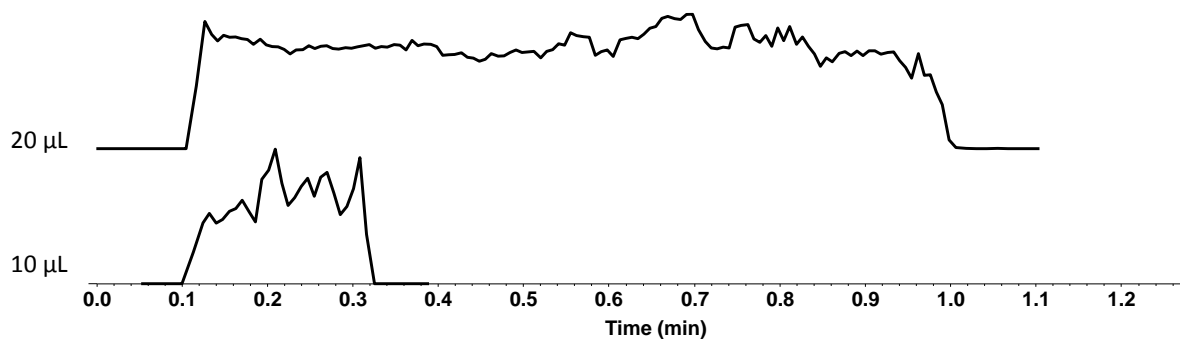


Figure S8. 500 ng/mL cocaine sprayed with 20 μL and 10 μL 100% acetonitrile with 3 kV spray voltage on un-waxed paper. When 10 μL spray solvent was used, signal lasted approximately 15 seconds, which was determined to be inadequate for more than one MS/MS observation. When the spray solvent volume was doubled, the signal lifetime was increased to nearly 1 minute, which was more suitable for calibration, as shown in **Fig. S7** above.

6. Duomeen detection in drum water. Water samples taken from pre- and post- treatment from a HP boiler system were analysed for the presence of Duomeen (m/z 325, **Figure S9**). Samples were analysed with 1 kV spray voltage and 10 μL MeOH/ H_2O (4:1, v/v).

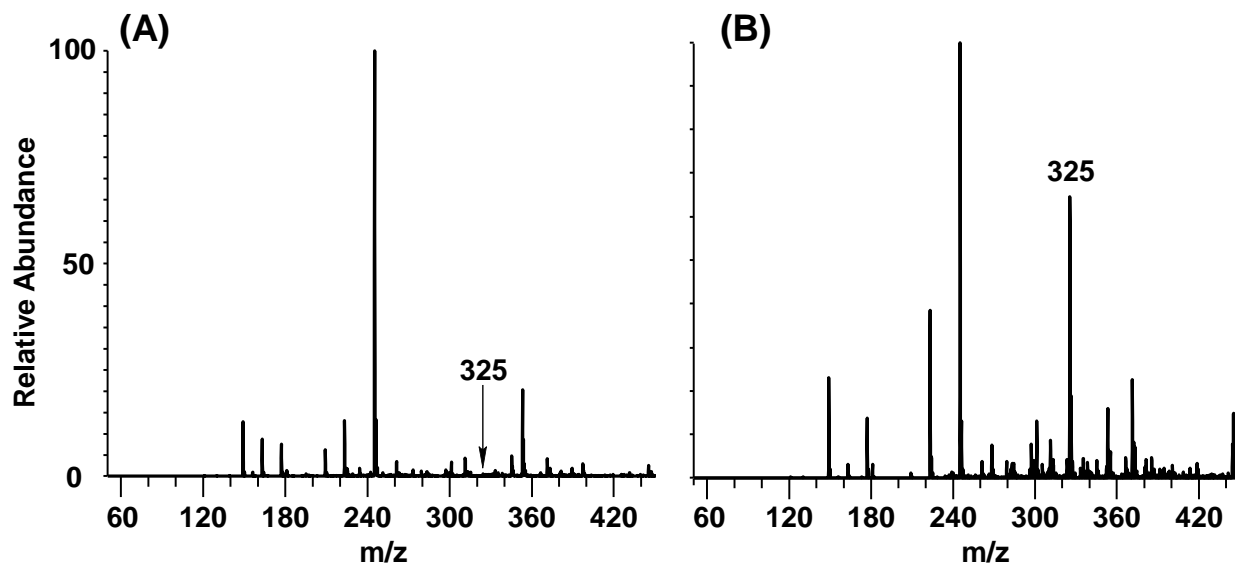


Figure S9. Analysis of water samples for detection of duomeen. Samples were taken from (A) pre-treatment, and (B) post-treatment stages in the boiler system cycle. Duomeen (m/z 325) was only detected in post-treatment sample, as expected.

7. Metaldehyde fragmentation in water samples. Analysis of water samples containing metaldehyde. 4 μL of 150 ng/mL metaldehyde sample was deposited onto wax paper and was then analysed with 10 μL 4:1 MeOH/H₂O spray solvent. Sodiated metaldehyde ions (m/z 199) were predominantly produced at 1 kV spray voltage whereas protonated ions (m/z 177) were observed at 3 kV. The fragmentation patterns for both ions are shown in **Fig S10**

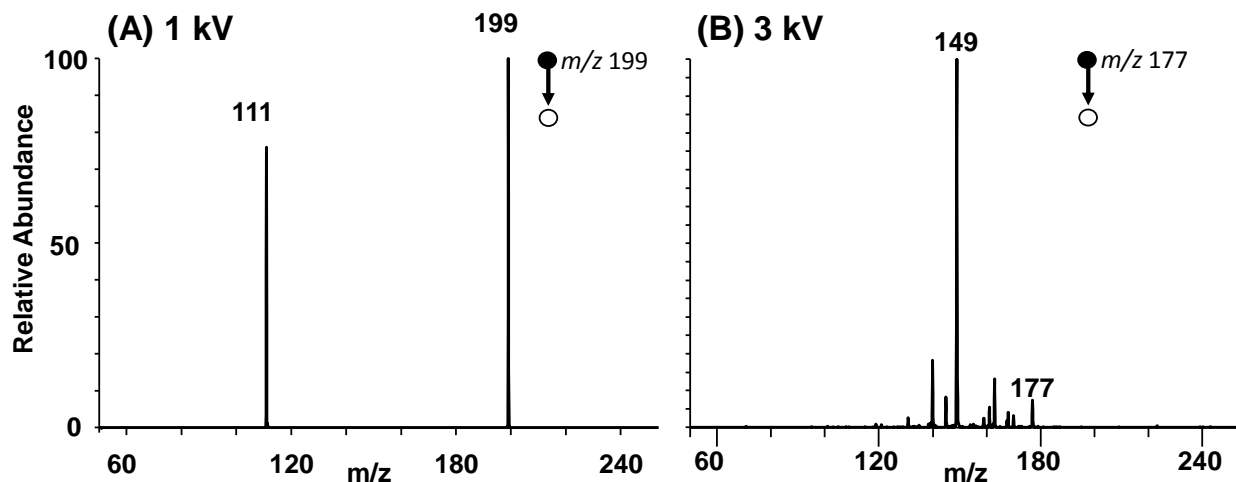


Figure S10. Analysis of water samples containing metaldehyde, sprayed at (A) analysis of 300 ng/mL sprayed at 1 kV, fragmentation m/z 199 $[\text{M}+\text{Na}]^+$, and (B) analysis of 150 ng/mL sprayed at 3 kV, fragmentation m/z 177 $[\text{M}+\text{H}]^+$. Intensities of fragment ions at m/z 111 and 149 were used to construct calibration curves found in Fig. 5 C and D, respectively.

8. Metaldehyde decomposition in acidified samples. Metaldehyde solutions prepared at pH 7 and 3 were analysed using paper spray. At solution pH 7, metaldehyde was ionized through sodium adduction yielding $[M+Na]^+$ ions (**Fig. 11A**). On the contrary, a peak at m/z 149 was detected from the acidified solution analysed after 5 min of preparation solution (**Fig. 11B**). This ion (m/z 149) is realized as due to the elimination of ethylene from protonated metaldehyde. The expectation is confirmed in gas-phase MS/MS experiment where the same fragmentation pathway was observed.

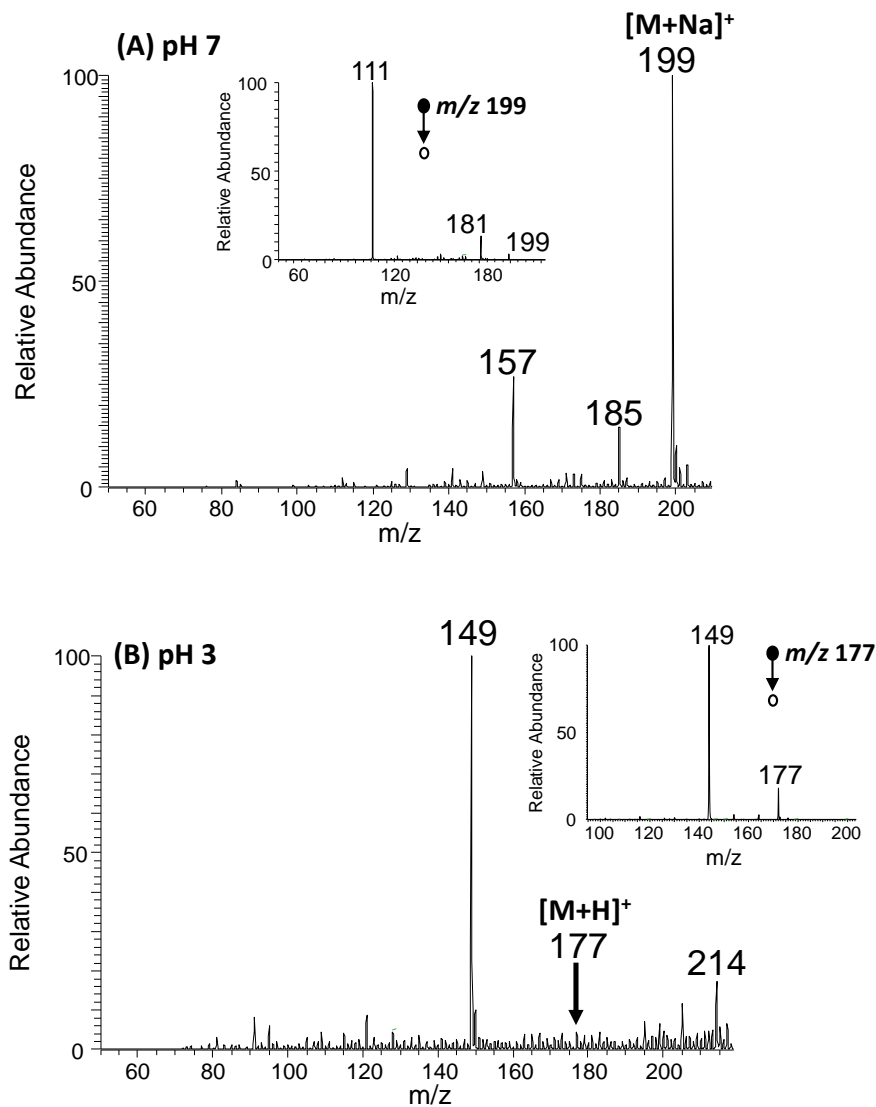


Figure 11. Comparison of PS-MS mass spectra for metaldehyde recorded at different pHs of (A) 7, and (B) 3. Spectrum in B was recorded after 5 min of adding acid. Inserts show product ion mass spectra for $[M+Na]^+$ at m/z 199 and for $[M+H]^+$ at m/z 177 achieved using collision-induced dissociation.